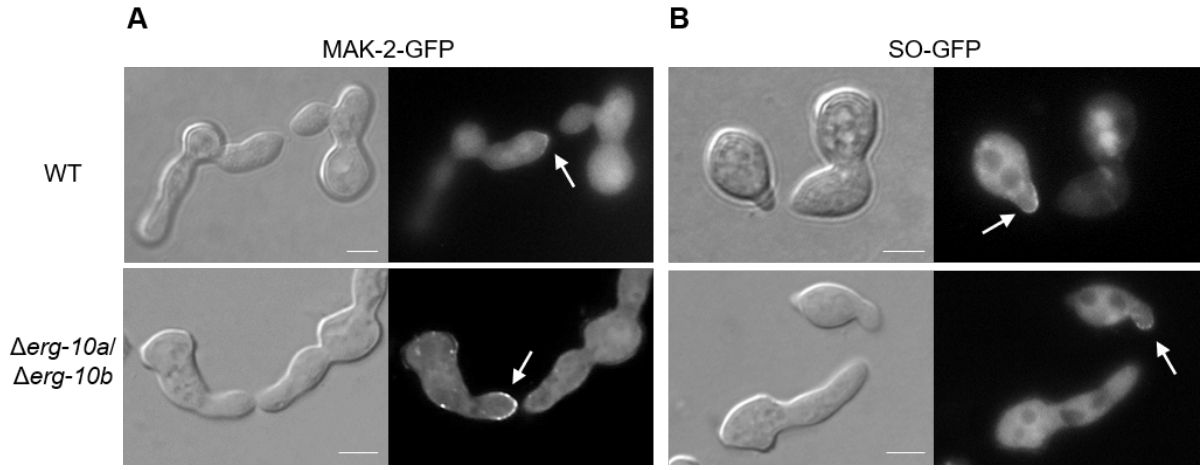

Figure S1 Interacting germlings of Δ*erg-10a*/Δ*erg-10b* show normal membrane recruitment of the signaling proteins MAK-2 and SO. (A) MAK-2-GFP localizes to one of the two cell tips of interacting WT (N1-41) and Δ*erg-10a*/Δ*erg-10b* (MW_220) germling pairs (arrows). (B) Similar to WT (AF-T8), SO-GFP also localizes to one of the two interacting germling tips in Δ*erg-10a*/Δ*erg-10b* (MW_223) (arrows). Scale bars: 5 µm.

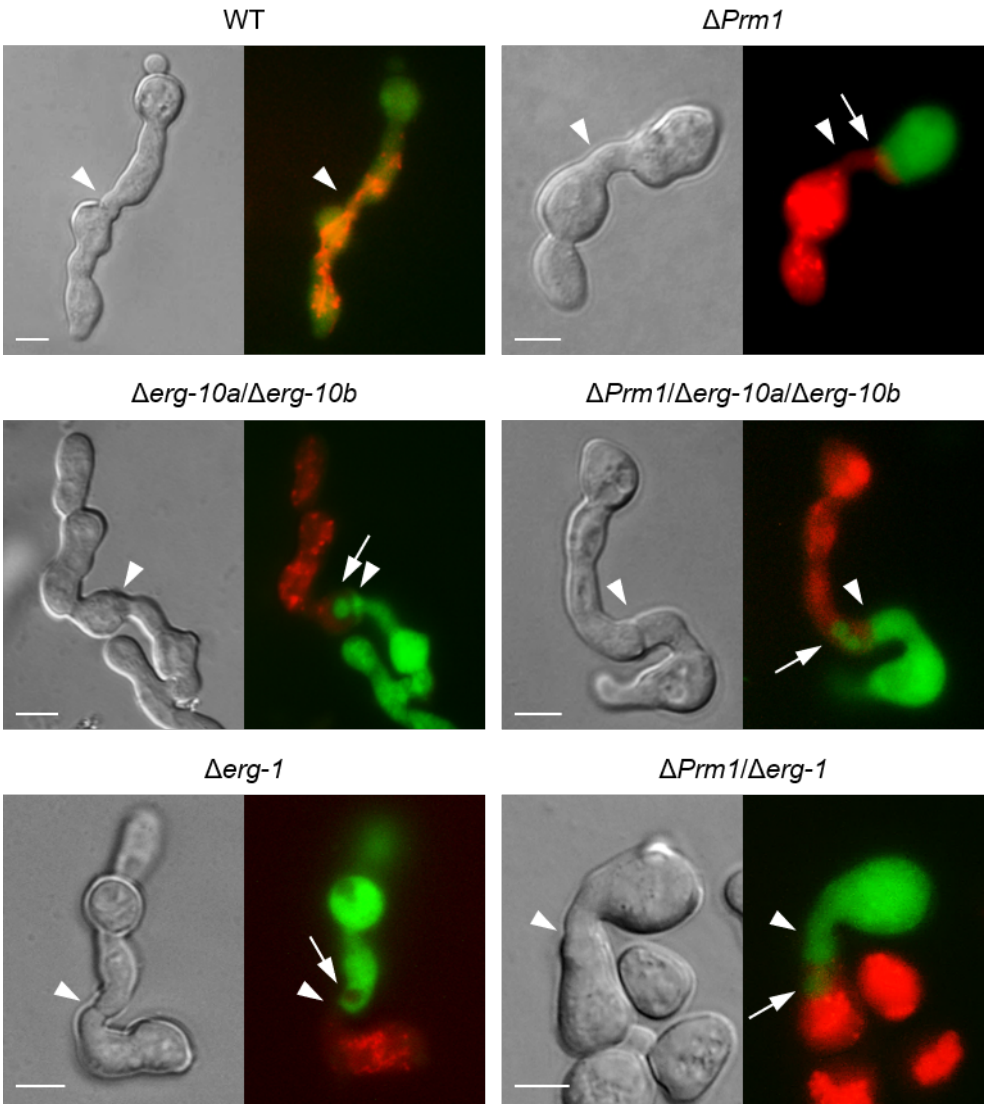

Figure S2 Germlings of the mutants Δ*Prm1*, Δ*erg-10a* Δ*erg-10b* and Δ*erg-1* are defective in cell-cell fusion. Germlings of WT and mutant strains expressing cytosolic green and red fluorescing proteins were analyzed for fusion between the interaction partners after physical contact (arrowheads). In contrast to normal fusion in WT cell pairs (N3-06 + N3-07), the cell contents of two germlings of the plasma membrane fusion mutant Δ*Prm1* (A7 + A8) are typically pushed into each other without mixing of the fluorescence colors (arrows). Germling pairs of the sterol biosynthesis mutants Δ*erg-10a*/Δ*erg-10b* (MW_175 + MW_179) and Δ*erg-1* (MW_463 + MW_465) show similar fusion deficiencies. Combining Δ*Prm1* with the deletion of the *erg* genes (MW_289 + MW_291; MW_459 + MW_455) results in comparable germling fusion defects. Scale bars: 5 µm.

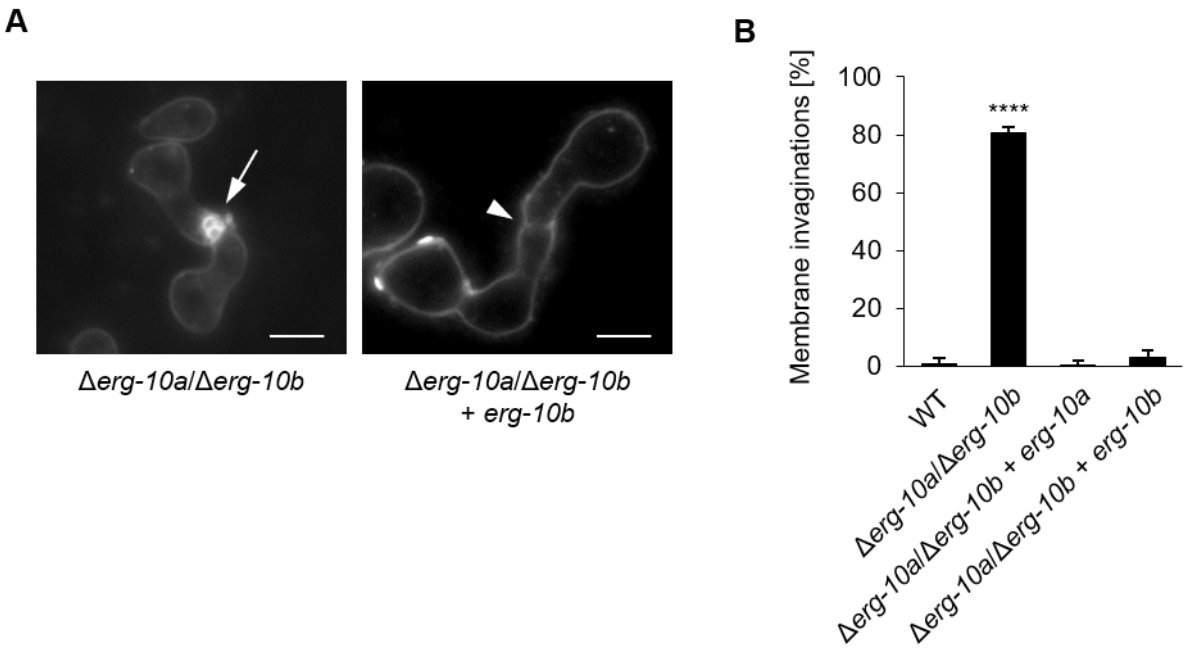

Figure S3 Complementation of Δ*erg-10a*/Δ*erg-10b*. (A) Fluorescence microscopy images of germling pairs of Δ*erg-10a*/Δ*erg-10b* (N4-38) and Δ*erg-10a*/Δ*erg-10b* + *erg-10b* (MW_631) stained with FM4-64. In contrast to the typical formation of membrane invaginations in cell pairs of the double mutant (arrow), the complemented strain forms a fusion pore between the fusion partners (arrowhead). Scale bars: 5 µm. (B) Quantification of membrane invaginations between germling pairs. While the vast majority of Δ*erg-10a*/Δ*erg-10b* cell pairs is characterized by membrane fingers as observed in A, these structures are rarely formed in WT (FGSC 2489) and the complemented strains (MW_630, MW_631). Values represent the mean ± SD from three independent experiments with 100 cell pairs per replicate (**** $P < 0.0001$, ANOVA with Tukey's post-hoc test).

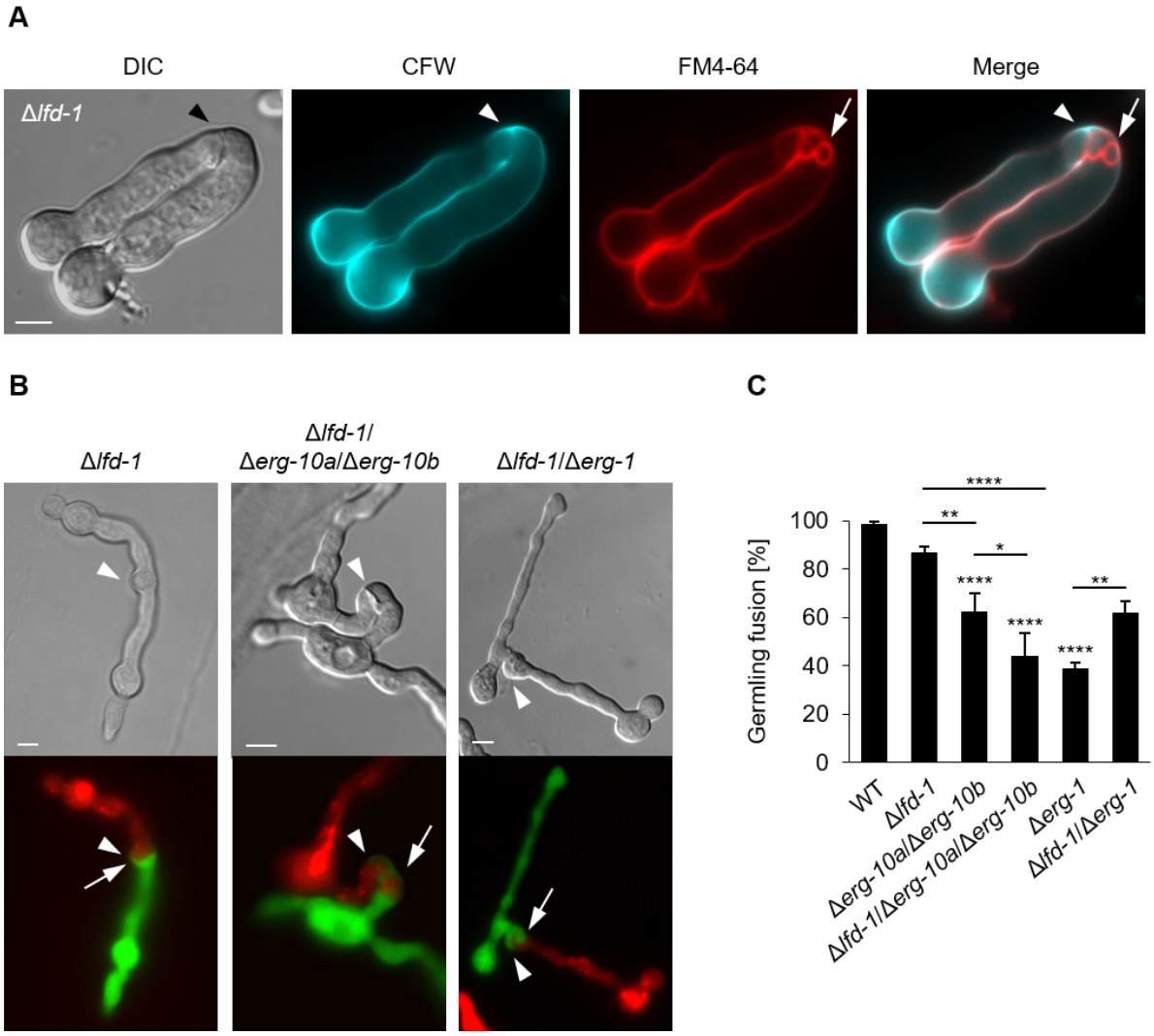

Figure S4 LFD-1 functions independently of ERG-10a, ERG-10b, and ERG-1. (A) Simultaneous staining of the cell wall with calcofluor white (CFW) and the cell membrane with FM4-64 in a pair of Δ*lfd-1* germlings (JPG6). The plasma membrane fusion defect of this mutant becomes visible by a membrane invagination (arrow) across the opening in the cell wall (white arrowhead) at the contact site (black arrowhead) of the cell pair. (B) Brightfield and fluorescence images of germling pairs lacking the plasma membrane fusion protein LFD-1 (JPG7 + JPG8), and cell pairs with the additional deletion of the ergosterol biosynthesis genes *erg-10a* and *erg-10b* (MW_623 + MW_626) or *erg-1* (MW_614 + MW_620). Due to the failure in plasma membrane merger, membrane invaginations (arrows) reach from one cell across the contact site (arrowheads) into the partner cell. Scale bars in A-B: 5 µm. (C) Quantification of germling fusion in cell pairs of WT (N3-06 + N3-07), Δ*lfd-1*, Δ*erg-10a*/Δ*erg-10b* (MW_175 + MW_179), Δ*lfd-1*/Δ*erg-10a* /Δ*erg-10b*, Δ*erg-1* (MW_463 + MW_465) and Δ*lfd-1*/Δ*erg-1*. Values represent the mean ± SD from three independent populations of germlings with 17 to 84 cells per replicate (* $P < 0.05$, ** $P < 0.01$, **** $P < 0.0001$, ANOVA with Tukey's post-hoc test).

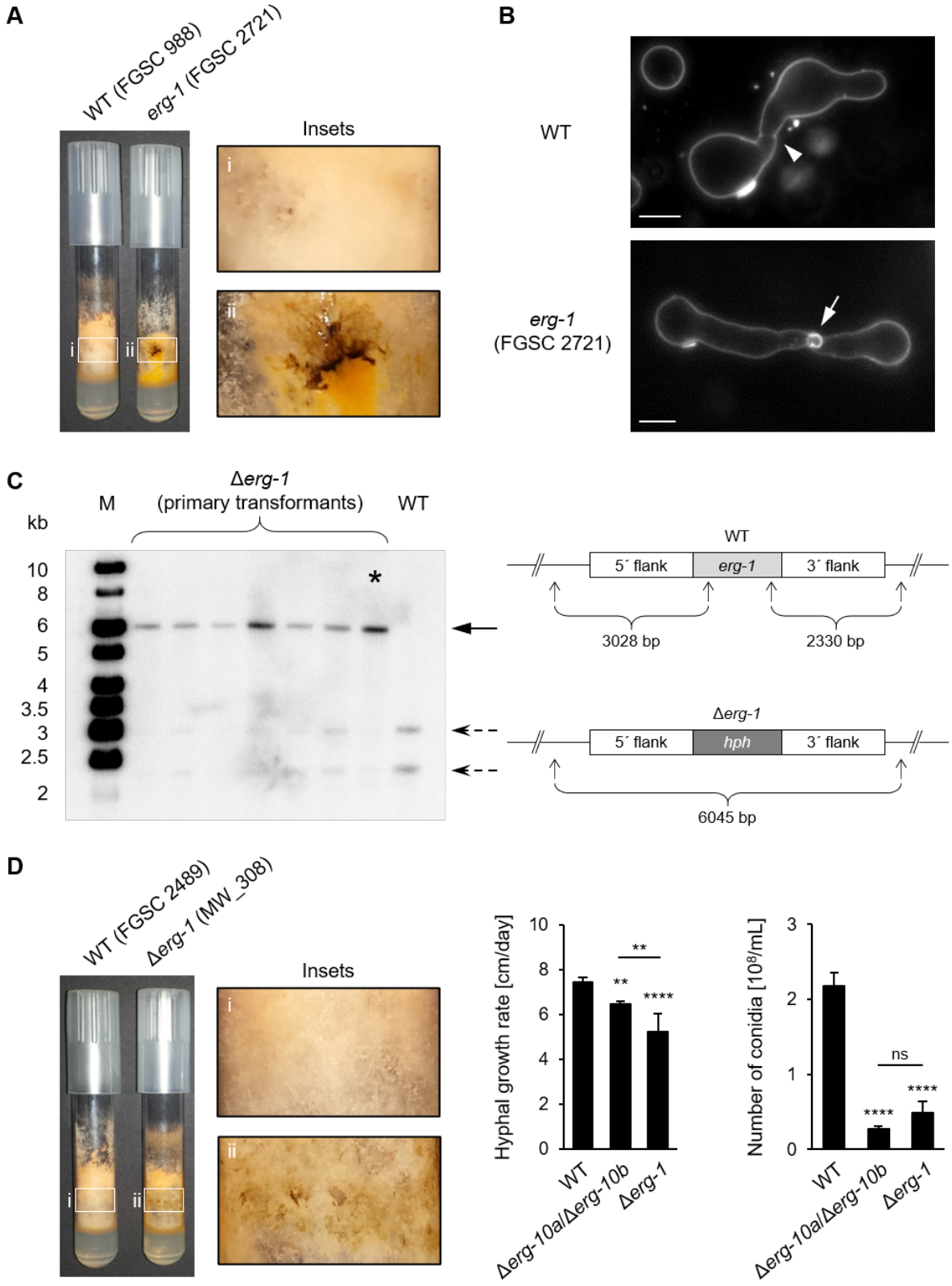

Figure S5 Construction and phenotypic characterization of the *erg-1* gene deletion mutant. (A) Growth of a classical *erg-1* mutant in comparison to a WT in flasks containing MM, showing dark pigmentation along the aerial mycelium. (B) Fluorescence microscopy images showing the staining of germling pairs with FM4-64. In contrast to the formation of a fusion pore (arrowhead) between WT germlings

(FGSC 2489), cell pairs of the classical *erg-1* mutant frequently form membrane invaginations after contact (arrow). Scale bars: 5 µm. (C) Southern blot analysis of primary transformants for the deletion of *erg-1* in strain FGSC 9719. Genomic DNA of seven mutants and a WT control (FGSC 988) was digested by XhoI, transferred onto a nylon membrane and hybridized with a radioactive probe derived from the entire gene knock-out cassette (left panel). As illustrated by schematic representations of the genomic regions of the gene in WT and Δ*erg-1* (right panels, not to scale), the detection of a signal at about 6 kb indicates gene replacement by a hygromycin resistance gene (*hph*) cassette (black arrow). Signals at about 2.3 and 3 kb in the transformants indicate heterokaryotic strains still containing WT nuclei (dotted arrows). Arrows below the genomic sequences depict XhoI restriction sites in the WT and the mutant. One of the isolated primary transformants (strain N3-08, asterisk) was chosen for purification into a homokaryon, resulting in strain MW_308. (D) Growth phenotypes of the Δ*erg-1* mutant strain. Compared to a WT control, the Δ*erg-1* mutant typically forms dark pigments along the glass wall of the culture tube (insets). Deletion of *erg-1* also reduces linear hyphal growth rates and the formation of vegetative conidia similar to the Δ*erg-10a*/Δ*erg-10b* mutant (N4-38). Values represent the mean ± SD from three to five cultures per strain (** $P < 0.01$, **** $P < 0.0001$, ns: not significant, ANOVA with Tukey's post-hoc test).

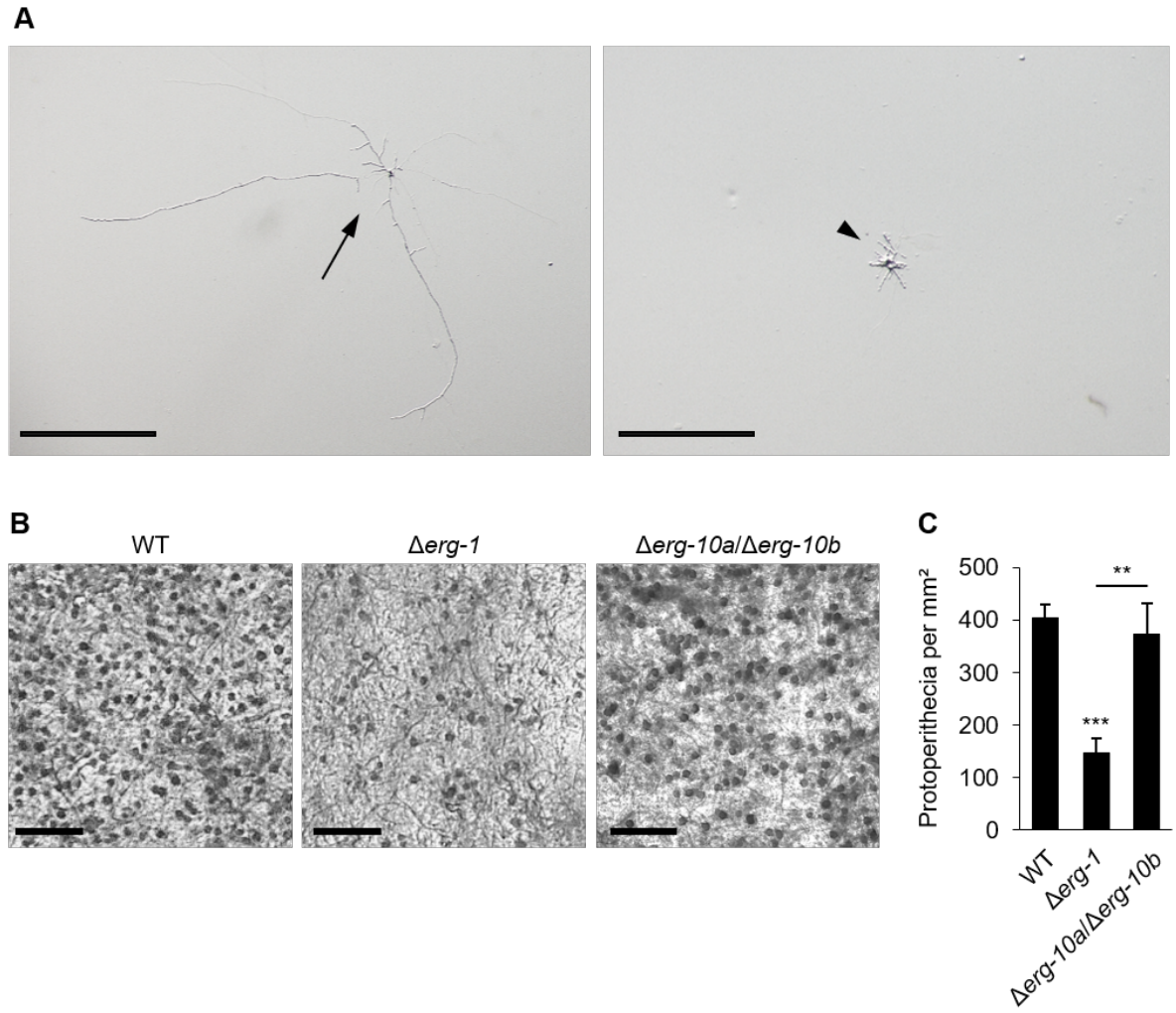

Figure S6 Deletion of *erg-1* impairs growth of ascospore germlings and the formation of protoperithecia. (A) Sexual crosses between WT (FGSC 2489) and Δ*erg-1* strains were used to purify the heterokaryotic *erg-1* gene deletion strain (MW_308) into a homokaryotic mutant. In a population of ascospores grown on MM plates, some microcolonies show strongly delayed growth (arrowhead) as compared to normally growing germlings (arrow). Diagnostic PCR analysis revealed that these slowly growing germlings are homokaryotic for Δ*erg-1* (data not shown). (B) Images of protoperithecia of WT (FGSC 988), Δ*erg-10a*/Δ*erg-10b* (N4-37) and Δ*erg-1* (MW_307) grown for one week on crossing medium. The deletion of *erg-1* reduces the number and size of these unfertilized fruiting bodies, while the lack of *erg-10a* and *erg-10* has no effect at this stage of development. Scale bars in A-B: 500 µm. (C) Quantitative evaluation of the number of protoperithecia generated by WT and *erg* mutants from representative images as shown in B. Values represent the mean ± SD from three independent cultures per strain (** $P < 0.01$, *** $P < 0.001$, ANOVA with Tukey's post-hoc test).

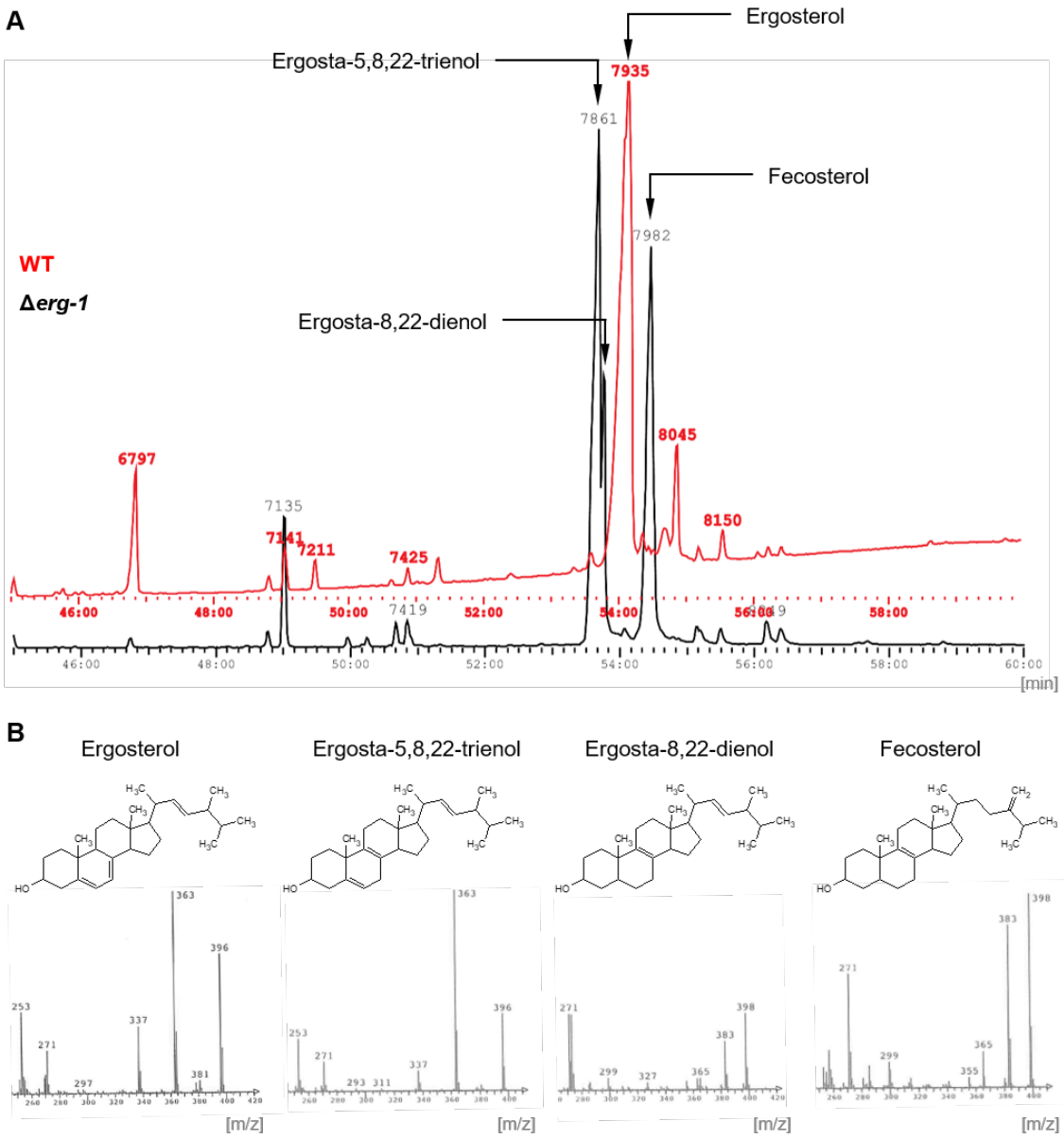

Figure S7 The ergosterol biosynthesis mutant Δ*erg-1* accumulates sterols with structural alterations in the ring system. Sterol extracts of WT (FGSC 2489) and Δ*erg-1* (MW_308) cultures were analyzed by gas chromatography coupled with mass spectrometry (GC/MS). (A) GC analysis of sterols extracts. In contrast to the main sterol in WT, which is ergosterol, the Δ*erg-1* mutant accumulates three sterol intermediates, identified as ergosta-5,8,22-trienol, ergosta-5,8-dienol and fecosterol (ergosta-8,24(28)-dienol). The horizontal scale represents the retention time of these sterols during the GC analysis. (B) Mass spectra and structures of the main sterols detected in WT and Δ*erg-1*. The scales represent mass over charge ratios of the fragments from the sterols that were detected in the GC analysis.

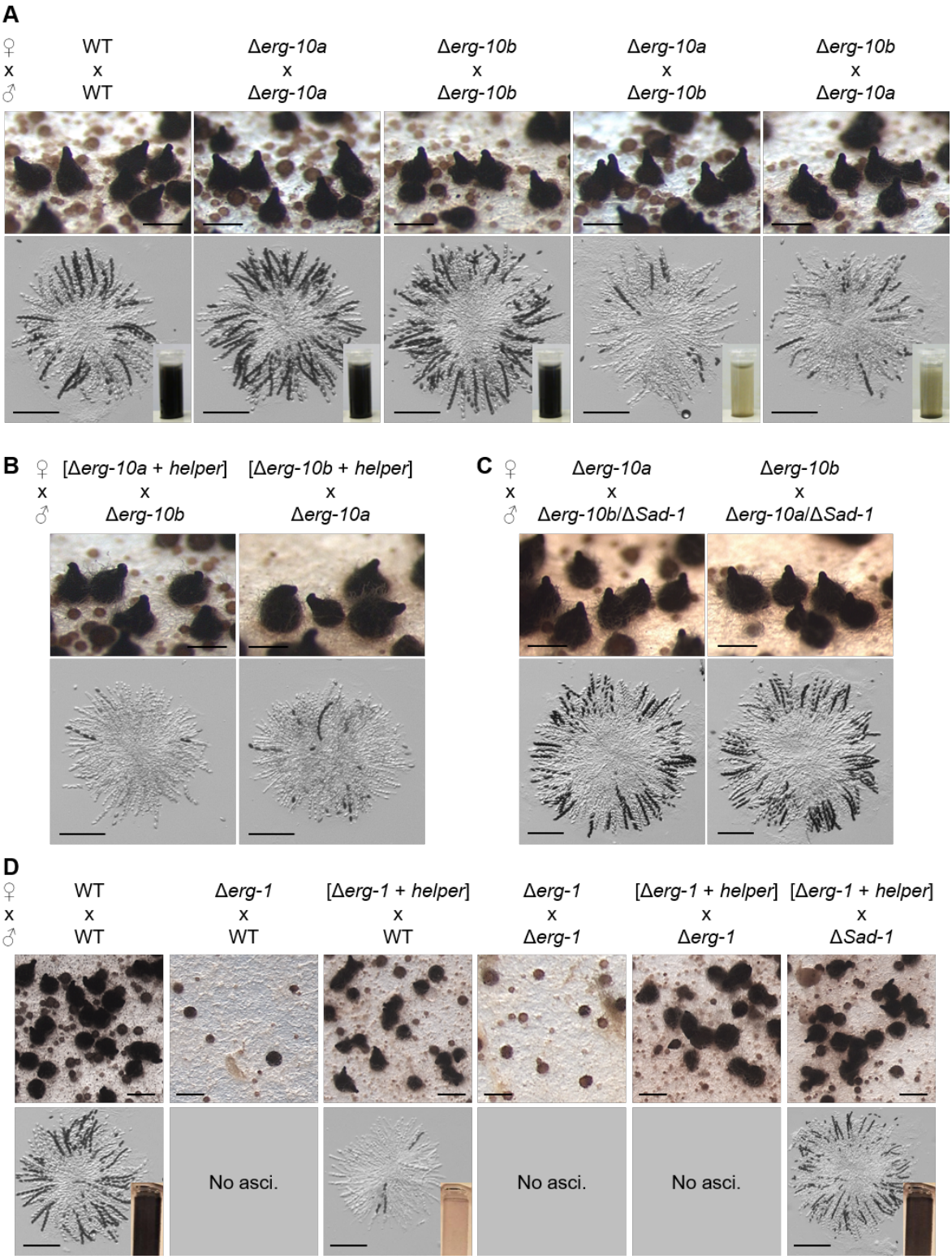

Figure S8 The reduced fertility of heterozygous crosses between Δ*erg-10a* and Δ*erg-10b* and the strong fertility defects of Δ*erg-1* are fully rescued by a combination of the *helper* strain and the suppressor Δ*Sad-1*. (A-C) Crosses (*mat a* x *mat A*) between WT (FGSC 2489, FGSC 988), Δ*erg-10a* (FGSC 20056, FGSC 20057) and Δ*erg-10b* (FGSC 13983, N4-30). (A) Heterozygous crosses between Δ*erg-10a* and Δ*erg-10b* produce WT-like fruiting bodies (top panels) and asci (bottom panels), but generate reduced amounts of black ascospores (inset images). (B)

Forced heterokaryons between the *helper* strain (FGSC 4564) and Δ*erg-10a* (MW_116) or Δ*erg-10b* (MW_185) do not rescue ascospore development in heterozygous crosses between these *erg* mutants. (C) The deletion of the suppressor *Sad-1* in one of the crossing partners (MW_209, MW_212) fully compensates for the impaired formation of ascospores in heterozygous crosses between Δ*erg-10a* and Δ*erg-10b*. (D) Crosses (*mat A* x *mat a*) between WT, Δ*erg-1* (MW_308, MW_307, MW_347), the *helper* strain and Δ*Sad-1* (FGSC 11151) were analyzed for the formation of perithecia, asci and ascospores. Homozygous crosses between Δ*erg-1* are infertile, which is not alleviated by using a forced heterokaryon with the *helper* strain. While crosses between the heterokaryon and WT are still defective, the additional use of Δ*Sad-1* as the male crossing partner fully restores female fertility of Δ*erg-1*. Scale bars: 500 µm for perithecia, 200 µm for rosettes of asci.

Table S1 Strains of *Neurospora crassa* used and constructed in this study.

Strain	Genotype	Origin
A7	Δ*Prm1*::*hph*, Δ*mus-51*::*bar*, *his-3*$^{+}$::P*ccg-1-gfp*, *mat A*	Fleissner *et al.* 2009
A8	Δ*Prm1*::*hph*, Δ*mus-51*::*bar*, *his-3*$^{+}$::P*ccg-1-dsRed*, *mat A*	Fleissner *et al.* 2009
A24	Δ*Prm1*::*hph*, Δ*mus-51*::*bar*, *his-3*$^{+}$::P*ccg-1-Prm1-gfp, mat A*	Fleissner *et al.* 2009
A32	Δ*Prm1*::*hph*, *mat A*	Fleissner *et al.* 2009
AF-T8	*his-3*$^{+}$::P*ccg-1-so-gfp*, *mat A*	Fleissner and Glass 2007
FGSC 988	*mat a*	FGSC
FGSC 2489	*mat A*	FGSC
FGSC 2721	*erg-1* (allele *uv1*), *mat A*	FGSC
FGSC 4564	*a*^{m1}, *ad-3B*, *cyh-1* (*helper* strain)	FGSC
FGSC 6103	*his-3*, *mat A*	FGSC
FGSC 9716	*his-3*, *mat a*	FGSC
FGSC 9719	Δ*mus-52*::*bar*, *mat a*	FGSC
FGSC 11151	Δ*Sad-1*::*hph*, *mat a*	FGSC
FGSC 11152	Δ*Sad-1*::*hph*, *mat A*	FGSC
FGSC 13983	Δ*erg-10b*::*hph*, *mat a*	FGSC
FGSC 20056	Δ*erg-10a*::*hph*, *mat a*	FGSC
FGSC 20057	Δ*erg-10a*::*hph*, *mat A*	FGSC
JPG6	Δ*lfd-1*::*hph*, *mat a*	Palma-Guerrero *et al.* 2014
JPG7	Δ*lfd-1*::*hph*, *his-3*$^{+}$::P*ccg-1-gfp*, *mat a*	Palma-Guerrero *et al.* 2014
JPG8	Δ*lfd-1*::*hph*, *his-3*$^{+}$::P*ccg-1-mCherry*, *mat a*	Palma-Guerrero *et al.* 2014
MW_103	Δ*erg-10b*::*hph*, *his-3*$^{+}$::P*ccg-1-gfp*, *mat A*	This study
MW_105	Δ*erg-10b*::*hph*, *his-3*$^{+}$::P*ccg-1-mCherry*, *mat A*	This study
MW_116	Δ*erg-10a*::*hph*, *his-3*, *mat A*	This study
MW_126	Δ*erg-10a*::*hph*, *Δerg-10b*::*hph*, *his-3*, *mat A*	This study
MW_149	Δ*erg-2*::*hph*, Δ*erg-11*::*hph*, *his-3*$^{+}$::P*ccg-1-gfp*, *mat A*	This study
MW_150	Δ*erg-2*::*hph*, Δ*erg-11*::*hph*, *his-3*$^{+}$::P*ccg-1-mCherry*, *mat A*	This study
MW_175	Δ*erg-10a*::*hph*, Δ*erg-10b*::*hph*, *his-3*$^{+}$::P*ccg-1-gfp*, *mat A*	This study
MW_179	Δ*erg-10a*::*hph*, Δ*erg-10b*::*hph*, *his-3*$^{+}$::P*ccg-1-mCherry*, *mat A*	This study
MW_181	Δ*erg-10a*::*hph*, Δ*erg-10b*::*hph*, *his-3*$^{+}$::P*ccg-1-gfp*, *mat A*	This study
MW_184	Δ*erg-10b*::*hph*, *his-3*, *mat A*	This study
MW_185	Δ*erg-10b*::*hph*, *his-3*, *mat a*	This study
MW_199	Δ*erg-10a*::*hph*, Δ*Prm1*::*hph*, *his-3*$^{+}$::P*ccg-1-Prm1-gfp*, *mat A*	This study

MW_209	Δ*erg-10a*::*hph*, Δ*Sad-1*::*hph*, *mat A*	This study
MW_212	Δ*erg-10b*::*hph*, Δ*Sad-1*::*hph*, *mat A*	This study
MW_220	Δ*erg-10a*::*hph*, Δ*erg-10b*::*hph*, *his-3*$^{+}$::P*ccg-1-mak-2-gfp*, *mat A*	This study
MW_223	Δ*erg-10a*::*hph*, Δ*erg-10b*::*hph*, *his-3*$^{+}$::P*ccg-1-so-gfp*, *mat A*	This study
MW_245	Δ*Prm1::hph*, *his-3*$^{+}$*::*P*ccg-1-Prm1-gfp*, *mat a*	This study
MW_275	Δ*erg-10a*::*hph*, Δ*Prm1*::*hph*, *his-3*$^{+}$::P*ccg-1-Prm1-gfp*, *mat a*	This study
MW_277.1	Δ*erg-10a::hph*, Δ*erg-10b::hph*, Δ*Prm1::hph his-3*, *mat A*	This study
MW_281	Δ*erg-10a*::*hph*, Δ*erg-10b*::*hph*, Δ*Prm1*::*hph*, *mat A*	This study
MW_289	Δ*erg-10a*::*hph*, Δ*erg-10b*::*hph*, Δ*Prm1*::*hph*, *his-3*$^{+}$::P*ccg-1-gfp*, *mat A*	This study
MW_291	Δ*erg-10a*::*hph*, Δ*erg-10b*::*hph*, Δ*Prm1*::*hph*, *his-3*$^{+}$::P*ccg-1-mCherry*, *mat A*	This study
MW_307	Δ*erg-1*::*hph*, *mat a*	This study
MW_308	Δ*erg-1*::*hph*, *mat A*	This study
MW_346	Δ*erg-1*::*hph*, *his-3*$^{+}$::P*ccg-1-h1-gfp*, *mat A*	This study
MW_347	Δ*erg-1*, *his-3*, *mat A*	This study
MW_368	Δ*erg-1*::*hph*, Δ*Prm1*::*hph*, *mat A*	This study
MW_450	Δ*erg-1*::*hph*, Δ*Prm1*::*hph*, *his-3*, *mat A*	This study
MW_455	Δ*erg-1*::*hph*, Δ*Prm1*::*hph*, *his-3*$^{+}$::P*ccg-1-mCherry*, *mat A*	This study
MW_459	Δ*erg-1*::*hph*, Δ*Prm1*::*hph*, *his-3*$^{+}$::P*ccg-1-gfp*, *mat A*	This study
MW_463	Δ*erg-1*::*hph*, *his-3*$^{+}$::P*ccg-1-gfp*, *mat A*	This study
MW_465	Δ*erg-1*::*hph*, *his-3*$^{+}$::P*ccg-1-mCherry*, *mat A*	This study
MW_614	Δ*erg-1*::*hph*, Δ*lfd-1*::*hph*, *his-3*$^{+}$::P*ccg-1-gfp*, *mat a*	This study
MW_620	Δ*erg-1*::*hph*, Δ*lfd-1*:*hph*, *his-3*$^{+}$::P*ccg-1-mCherry*, *mat a*	This study
MW_623	Δ*erg-10a*::*hph*, Δ*erg-10b*::*hph*, Δ*lfd-1*::*hph*, *his-3*$^{+}$::P*ccg-1-gfp*, *mat a*	This study
MW_626	Δ*erg-10a*::*hph*, Δ*erg-10b*::*hph*, Δ*lfd-1*::*hph*, *his-3*$^{+}$::P*ccg-1-mCherry*, *mat a*	This study
MW_630	Δ*erg-10a*::*hph*, Δ*erg-10b*::*hph*, *his-3*$^{+}$::P*ccg-1-erg-10a*, *mat A*	This study
MW_631	Δ*erg-10a*::*hph*, Δ*erg-10b*::*hph*, *his-3*$^{+}$::P*ccg-1-erg-10b*, *mat A*	This study
N1-41	*his-3*$^{+}$::P*ccg-1-mak-2-gfp*, *mat A*	Weichert *et al.* 2016
N2-12	*his-3*$^{+}$::P*ccg-1-h1-gfp*, *mat A*	Gift from D. J. Jacobson
N3-06	*his-3*$^{+}$::P*ccg-1-gfp*, *mat A*	Fleissner *et al.* 2009
N3-07	*his-3*$^{+}$::P*ccg-1-mCherry*, *mat A*	Schürg *et al.* 2012
N3-08	Δ*erg-1*::*hph*, Δ*mus-52*::*bar*, *mat a*	This study

N4-30	Δ*erg-10b*::*hph*, *mat A*	Weichert *et al.* 2016
N4-37	Δ*erg-10a*::*hph*, Δ*erg-10b*::*hph*, *mat a*	This study
N4-38	Δ*erg-10a*::*hph*, Δ*erg-10b*::*hph*, *mat A*	Weichert *et al.* 2016
N5-01	Δ*erg-10a*::*hph*, *his-3*$^{+}$::P*ccg-1-gfp*, *mat A*	This study
N5-02	Δ*erg-10a*::*hph*, *his-3*$^{+}$::P*ccg-1-mCherry*, *mat A*	This study
N5-03	Δ*erg-11*::*hph*, *his-3*$^{+}$::P*ccg-1-gfp*, *mat A*	This study
N5-04	Δ*erg-11*::*hph*, *his-3*$^{+}$::P*ccg-1-mCherry*, *mat A*	This study

Table S2 Oligonucleotides used in this study.

No.	Name	Nucleotide sequence (5´–3´)
21	his-3-f	CTTGCAGTCTTGCACGTTG
22	his-3-r	CTCTCGAGTCCCGTTATTGC
42	prm-f	ATTATTATCTAGAATGGTTTACAACGAAAAGAATGGAGG
43	prm-r	ATCATCATTAATTAATCCTCCTCCTCCTCCTCCAATAGGCGTAAAATACCC
82	HPH F	GTCGGAGACAGAAGATGATATTGAAGGAGC
83	HPH R	GTTGGAGATTTCAGTAACGTTAAGTGGAT
103	erg1-5F	GTAACGCCAGGGTTTTCCCAGTCACGACGCGTAGATCTTTACCCTGTCC
104	erg1-5R	ATCCACTTAACGTTACGTTACTGAAATCTCCAACCCAACCTCAACAAACCTACC
105	erg1-3F	CTCCTTCAATATCATCTTCTGTCTCCGACACCTTCGTAGAGAATGCACG
106	erg1-3R	GCGGATAACAATTTCACACAGGAAACACCCGGTAGTACTAAGCTGAACG
312	erg-1-test-f	TGGGATGCTTGCTTGTGATGCG
315	erg-10a-test-f	TTTCTGTGGGAGGGGAGATGTCTGG
317	hph-test-r	TCGTCCGAGGGCAAAGGAATAGAG
338	erg-1-f	CTCTTCCTCCGGTTCGTCTTGCC
339	erg-1-r	CAAGTTGCTAATCATCTCGCGGCCG
344	erg-10a-f	ACGACCTGCTCTCTATGATTTCCC
345	erg-10a-r	CTCCTTGACAATCTTCTCCATCTCG
386	erg-10b-test-f	GTAGAGCGATATGTAGGTGCTGGCC
387	erg-10b-f	GCTCCTATACTGGGTGTTTAGCG
388	erg-10b-r	CATGTGATGCAGTGTGTGGTGGG
417	prm1-test-f	TGAAGATGGTGAAGACGTCGG
569	sad-1-hph-test-f	ACTCGATTGGCTGGGGTAAGAAGG
576	sad-1-f	GGAACTCTTCAAGGATCATGCAGCC
577	sad-1-r	GGAACACCAAGAGACGAGAGAACGG
626	prm1-wt-test-r	AAGAGAGAGTGGGACTGGAGGG
676	erg-1-f-seq	GGTGGTGGAATCTCTGTGGCC
677	erg-1-r-seq	TCTAGCGTAGACGCCGCTTGTGC
1078	lfd-1-test-f	CGCAACCTCAACATATCATT
1079	lfd-1-f	ATGGCTGTCAACGTGAACGA
1080	lfd-1-r	TCAAGCATCTCCTGCATTCA
1445	erg-10a_Prom_PacI_F	AATGTATTAATTAAATTTTGTTATTGCCAACTTG
1446	erg-10a_Term_NotI_R	AATGTAGCGGCCGCGCTTATCTCCGGTTCAACGG
1447	erg-10b_Prom_PacI_F	AATGTATTAATTAAGCAGTATACACTAGGACTTA
1448	erg-10b_Term_NotI_R	AATGTAGCGGCCGCCTAAACCTCTCTGTTGTCTG